Atmos. Chem. Phys. Discuss., 13, 9267–9317, 2013
www.atmos-chem-phys-discuss.net/13/9267/2013/
doi:10.5194/acpd-13-9267-2013

Atmospheric Chemistry and Physics Discussions

Absorption properties of Mediterranean aerosols obtained from multi-year ground-based and satellite remote sensing observations

M. Mallet[1,2], O. Dubovik[3], P. Nabat[4], F. Dulac[5], R. Kahn[6], J. Sciare[5], D. Paronis[7], and J. F. Léon[1,2]

[1]Université de Toulouse, UPS, LA (Laboratoire d'Aérologie), 14 avenue Edouard Belin, 31400 Toulouse, France
[2]CNRS, LA (Laboratoire d'Aérologie), UMR5560, 31400 Toulouse, France
[3]Laboratoire d'Optique Atmosphérique, Lille, France
[4]CNRM-GAME, Météo-France, Toulouse, France
[5]Laboratoire des Sciences du Climat et de l'Environnement (IPSL/LSCE), CEA-CNRS-USVQ, Gif-sur-Yvette, France
[6]NASA Goddard Space Flight Center, Maryland, USA
[7]National Observatory of Athens, Institute for Astronomy, Astrophysics, Space Applications and Remote Sensing, Athens, Greece

Received: 12 February 2013 – Accepted: 18 March 2013 – Published: 8 April 2013

Correspondence to: M. Mallet (marc.mallet@aero.obs-mip.fr)

Published by Copernicus Publications on behalf of the European Geosciences Union.

Discussion Paper | Discussion Paper | Discussion Paper | Discussion Paper |

Abstract

Aerosol absorption properties are of high importance to assess aerosol impact on regional climate. This study presents an analysis of aerosol absorption products obtained over the Mediterranean Basin or land stations in the region from multi-year ground-based AERONET and satellite observations with a focus on the Absorbing Aerosol Optical Depth (AAOD), Single Scattering Albedo (SSA) and their spectral dependence. The AAOD and Absorption Angström Exponent (AAE) data set is composed of daily averaged AERONET level 2 data from a total of 22 Mediterranean stations having long time series, mainly under the influence of urban-industrial aerosols and/or soil dust. This data set covers the 17 yr period 1996–2012 with most data being from 2003–2011 (~89 % of level-2 AAOD data). Since AERONET level-2 absorption products require a high aerosol load (AOD at 440 nm > 0.4), which is most often related to the presence of desert dust, we also consider level-1.5 SSA data, despite their higher uncertainty, and filter out data with an Angström exponent <1.0 in order to study absorption by carbonaceous aerosols. The SSA data set includes both AERONET level-2 and satellite level-3 products. Satellite-derived SSA data considered are monthly level 3 products mapped at the regional scale for the spring and summer seasons that exhibit the largest aerosol loads. The satellite SSA dataset includes the following products: (i) Multi-angle Imaging SpectroRadiometer (MISR) over 2000–2011, (ii) Ozone Monitoring Instrument (OMI) near-UV algorithm over 2004–2010, and (iii) MODerate resolution Imaging Spectroradiometer (MODIS) Deep-Blue algorithm over 2005–2011, derived only over land in dusty conditions. Sun-photometer observations show that values of AAOD at 440 nm vary between 0.024 ± 0.01 (resp. 0.040 ± 0.01) and 0.050 ± 0.01 (0.055 ± 0.01) for urban (dusty) sites. Analysis shows that the Mediterranean urban-industrial aerosols appear "moderately" absorbing with values of SSA close to [redacted]0.94–0.95 ± 0.04 (at 440 nm) in most cases except over the large cities of Rome and Athens, where aerosol appears more absorbing (SSA ~0.89–0.90 ± 0.04). The aerosol Absorption Angström Exponent (AAE estimated using 440 and 870 nm) is found to be larger than 1 for most sites over

the Mediterranean, a manifestation of mineral dust (iron) and/or brown carbon producing the observed absorption. AERONET level-2 sun-photometer data indicate the existence of a moderate East–West gradient, with higher values over the eastern basin ($AAE_{East.}$ = 1.39/$AAE_{West.}$ = 1.33) due to the influence of desert dust. The North–South AAE gradient is more pronounced, especially over the western basin. Our additional analysis of AERONET level-1.5 data also shows that organic absorbing aerosols significantly affect some Mediterranean sites. These results indicate that current climate models treating organics as nonabsorbing over the Mediterranean certainly underestimate the warming effect due to carbonaceous aerosols. A comparative analysis of the regional SSA variability has been attempted using satellite data. OMI and MODIS data show an absorbing zone (SSA ~0.90 at 470–500 nm) over Northeastern Africa that does not appear in the MISR retrievals. In contrast, MISR seems able to observe the East–West SSA gradient during summer, as also detected by AERONET. Also, the analysis of SSA provided by satellites indicates that the aerosol over the Mediterranean Sea appears less absorbing during spring (MAM) than summer (JJA).

1 Introduction

Numerous studies have identified the Mediterranean basin as one of the most prominent "Hot-Spots" in projected climate change assessments (Giorgi, 2006, Giorgi and Lionello, 2008). General Circulation Model (GCM) or Regional Climate Model (RCM) [redacted] simulations have demonstrated that the Mediterranean is characterized by its vulnerability to changes in the water cycle and predict a substantial precipitation decrease and warming, especially during the summer season. By the end of 21 century, the average prediction of the models suggests a significant loss of freshwater over the Mediterranean basin: −40 % for the period 2070–2090 compared to 1950–1999 (Sanchez-Gomez et al., 2009). Climate simulations underline that the drying of the Mediterranean basin is associated with increasing anticyclonic circulation over the

region, which causes a northward shift of the mid-latitude storm track (Giorgi and Lionello, 2008).

Until now, most global and regional future climate simulations have only investigated the impact of global warming on the Mediterranean climate without clearly considering the influence of "Mediterranean aerosols" (pollution particles, smoke and mineral dust) that can significantly modify the radiation budget (Markowicz et al., 2002; Formenti et al., 2002b; Mallet et al., 2006; Roger et al., 2006). Specifically, atmospheric aerosols decrease the amount of shortwave (SW) radiation reaching the sea and continental surfaces. The column amount of atmospheric aerosol, quantified by the Aerosol Optical Depth (AOD), is one of the main factors causing this decrease. This aerosol-induced perturbation of the surface radiation budget can impact the Sea Surface Temperature (SST) (Foltz and McPhaden, 2008; Yue et al., 2011) and surface moisture exchanges by modifying latent heat fluxes (Ramanathan et al., 2001a).

In addition, due to their optical properties and especially their ability to absorb solar radiation, aerosols can trap SW radiation within the atmospheric layer where they reside. This additional absorption contributes to the direct heating of the atmosphere and causes changes in the atmospheric heating rate profiles, dynamical processes and more generally, the hydrological cycle (Solmon et al., 2008; Lau et al., 2009; Mallet et al., 2009). For example, Solmon et al. (2008) simulate that a change in dust absorbing properties could modify precipitation over Western Africa. Ramanathan et al. (2001b) also conclude that heating caused by carbonaceous absorbing aerosols exported from India reduces the low cloud fraction over the Indian Ocean during the dry monsoon season. Therefore, a rigorous quantification of the effect of aerosols on the Mediterranean radiation budget and climate is required, including estimates of both the atmospheric aerosol load and its ability to absorb radiation.

Numerous studies of aerosol properties over the Mediterranean have documented AOD for pollution particles, smoke and dust aerosols using in-situ observations (Horvath et al., 2002; Formenti et al., 2002; Gerasopoulos et al., 2003; Kubilay et al., 2003; Meloni et al., 2004, 2006; Fotiadi et al., 2006; Pace et al., 2006; Roger et al., 2006;

Mallet et al., 2006; Tafuro et al., 2007; Saha et al., 2008). In brief, these studies report AOD values in the range 0.1–0.5, 0.3–1.8 and 0.3–0.8 in the spectral range of 440 to 550 nm for pollution, dust and smoke particles, respectively. In addition to analyses of local sun-photometer observations, several studies have used long time series of satellite-derived AOD at regional scales from Meteosat (Moulin et al., 1998), SeaWiFs (Antoine and Nobileau, 2006), the MODerate resolution Imaging Spectroradiometer (MODIS) (Barnaba and Gobbi, 2001; Papadimas et al., 2008, 2009; Nabat et al., 2012), the combination of MODIS and TOMS (Hatzianastassiou et al., 2009), MSG/SEVIRI (Lionello et al., 2012), or even all products (Nabat et al., 2012).

In contrast to the considerable scientific literature related to AOD distribution, aerosol absorbing properties over the Mediterranean have received much less attention, and are poorly documented, in spite of their great importance for direct radiative forcing and overall regional climate. To the best of our knowledge, the only long term in-situ observations of absorbing aerosols available in the Mediterranean background atmosphere are those reported from Crete Island in the eastern Mediterranean by Sciare et al. (2008), highlighting the major role of long-range transported biomass burning aerosols on Black Carbon (BC) concentration levels. Consequently, long-term observations of absorption in the atmospheric column, and specifically an analysis of the role played by dust aerosols, are still missing. In addition, aerosol single scattering albedo (SSA) products now available from several satellite missions (Hsu et al., 2004; Torres et al., 2007; Kahn et al., 2010) have not yet been analysed over the Mediterranean. This motivates the present work; its main objective is to characterise aerosol absorption over the Mediterranean region using available surface and satellites remote sensing data. We focus our study on (i) the aerosol absorption optical depth (AAOD), which is the fraction of AOD due to absorption only, (ii) the aerosol single scattering albedo (SSA), which is the ratio of aerosol scattering to total extinction (i.e. scattering + absorption), and (iii) the spectral dependence of these optical parameters, calculated in terms of Angström Exponent (AE) or Absorption Angström Exponent (AAE) in the case of optical depth or

absorption optical depth, respectively:

$$AE = \log(AOD_{\lambda 1}/AOD_{\lambda 2})/\log(\lambda_2/\lambda_1) \text{ and } AAE = \log(AAOD_{\lambda 1}/AAOD_{\lambda 2})/\log(\lambda_2/\lambda_1) \quad (1)$$

Subsequent to the data description (ground-based and satellite remote sensing data set used in our work) in Sect. 2, the results are presented and discussed in two main parts. First (Part 3.1–3.2), we report AAOD and AAE AERONET level-2 and 1.5 multi-year observations for different Mediterranean sites. In a second time (Part 3.3), we exploit AERONET but also satellite SSA products derived at the regional scale from the Ozone Monitoring Instrument (OMI) (Torres et al., 2007), MODIS (Deep Blue algorithm; Hsu et al., 2004, 2006) and the Multi-angle Imaging SpectroRadiometer (MISR) (Kahn et al., 2010). Our analysis of satellite data is focused on the summer (June-July-August, JJA) and spring (March-April-May, MAM) periods, corresponding to the presence of the main Mediterranean aerosols (pollution particles, smoke and mineral dust; Barnaba et al., 2004) and highest AOD over the basin (Nabat et al., 2012).

2 Remote sensing ground-based and satellite observations

2.1 Surface AERONET observations

AERONET (Aerosol Robotic Network; http://aeronet.gsfc.nasa.gov/) is a federated network of ground-based sun-photometers and the associated data inversion and archive system, that routinely performs direct sun observations every 15 mn, and both almucantar and principal plane sky radiance measurements, and retrieves and distributes global aerosol columnar properties (Holben et al., 1998). Along with AOD observations, the AERONET aerosol retrieval algorithm (Dubovik and King, 2000) delivers the complete set of column-effective aerosol microphysical parameters, including volume size distribution, refractive index at four wavelengths (440, 670, 870 and 1020 nm) and fraction of spherical particles (Dubovik et al., 2006, also see description in Dubovik et al., 2011). In addition, using these microphysical parameters, the algorithm provides other

column-effective aerosol optical properties of interest to the scientific community, such as wavelength dependent SSA, phase function, and asymmetry parameter, as well as integral parameters of bi-modal particle size distributions (concentration, mode radii and variances) (Dubovik et al., 2002). In the present study, the analysis is mostly focused on AAOD and SSA for AERONET level 2.0, cloud-screened and quality-assured AOD (Smirnov et al., 2000) and level 2.0 inversion products (Dubovik et al., 2002). The accuracy of AERONET retrievals is evaluated and discussed by Dubovik et al. (2000, 2002): the uncertainty of retrieved AAOD is estimated at the level of ±0.01 at wavelengths 440 nm and greater, whereas SSA uncertainty is estimated to be ±0.03 for AOD > 0.2 and ±0.07 for AOD < 0.2 (Dubovik et al., 2000, 2002).

The 22 AERONET Mediterranean sites considered in our study are selected based on both their location (within or close to the basin) and their long term operation (> 2.5 years). They are mapped in Fig. 1 and listed in Table 1 along with information regarding the location, period of observation and a brief description of each site. The significant number of AERONET sites available over the Mediterranean and their distribution allows us to investigate aerosol characteristics under diverse conditions: over remote, anthropogenic-polluted and dusty locations. Figure 2 plots averaged level-2 AE and AOD of the different stations. The 4 stations of Thessaloniki, Erdemli, Nes Ziona and Modena show a high AOD range (0.28–0.32) whereas all other have an average < 0.23. The high AE (~ 1.55) at Modena and Thessaloniki indicate urban pollution controlled by submicron particles. On the opposite, the low average AE value (< 1.0) at Nes Ziona reveals the major influence of large particles, likely soil dust and possibly sea salt. Lampedusa, Blida and Sede Boker also show a low AE (~ 1), characterising a major influence of large particles in conditions of lower AOD (~ 0.2). With intermediate AE values in the range 1.11–1.27 the stations of Malaga, Granada, Oristano, Forth Crete and Erdemli correspond to relatively southern stations (Fig. 1) where the influence of desert dust from the south is still very significant. Larger AE values in the range 1.31–1.37 correspond to stations in a latitude band 38–40.6° N (Burjassot, Potenza, Lecce, Messina and Athens) where the impact of dust is less visible but still signifi-

cant. The rest of the stations has an AE in the range 1.41–1.49 and is composed of more northern stations in the western basin (Barcelona, Rome, Avignon, Ersa, Toulon, and Villefranche). As a result, a very significant trend is found between AE and station latitude, whereas AOD rather correlates with the station longitude (Fig. 3).

Figure 4 provides the temporal distribution of the number of days per month with AERONET level-2 absorption products available at each site considered. Numbers are most often < 10 and this number is rarely exceeded at other seasons than summer. The period covered spans from 1996 to 2012 but a single station of Sede Boker provides data before 2000. Figure 5 further plots some statistics. Twelve stations have at least 110 days of level-2 absorption products. The number ranges between 18 and 365 days (at Ersa and Erdemli, resp.) and the maximum number of days is always found in the summer season which is known to be the maximum dust season in the western and central Mediterranean (Moulin et al., 1998). 88.8 % of data are from the period 2003–2011. As AERONET level-2 derivations correspond to a high aerosol load (AOD at 440 nm > 0.4) that is generally associated to dust events, we also consider level-1.5 inversion products in order to investigate the possible role of smoke aerosols on the absorption. We further limit the influence of dust events on the results by considering only level-1.5 data with an Angström Exponent > 1.0. In that case, uncertainties on AAOD are estimated at about ±0.01.

2.2 Satellite MISR observations

The MISR sensor aboard the NASA-Earth Observing System (EOS) Terra satellite provides estimates of AOD and SSA using top-of-atmosphere radiance measurements in four spectral channels (446, 558, 672 and 867 nm, Table 3) in each of nine different viewing angles (nadir plus 26.1°, 45.6°, 60.0°, and 70.5° in the forward and aft directions along the spacecraft track). The spatial resolution of the MISR Standard version 22 (V22) aerosol products is 17.6 km, and the level 3 aggregated product used here is reported at 0.5°. A detailed description of SSA retrievals is given in Kahn et al. (2010, and references therein). Here, we used MISR SSA values derived at 558 nm

(Table 3). The key advantage of the MISR measurement approach is the use of different geometric views, making it possible to retrieve aerosol properties while accounting self-consistently for surface reflectance (Martonchik et al., 2009) and avoiding sunglint. Here, we consider the monthly level-3 data "MIL3DAE" products version F15_0031 for the period 2000 to 2011 (Table 3). As mentioned below, we focus our analysis on the spring (MAM) and summer (JJA) seasons, when the major aerosol loading occurs over the Mediterranean basin. It should be remembered that MISR SSA values are categorical rather than quantitative (two-to-four bins under good retrieval conditions – e.g. "absorbing" and "non-absorbing"), and the quality of the value depends on retrieval conditions, such as AOD (Kahn et al., 2010). As such, MISR-retrieved SSA is useful mainly for making qualitative distinctions among adjacent air masses containing aerosols having different SSA values (e.g. Kahn et al., 2009). In that sense, the aim of this work is to propose a first analysis of the SSA regional patterns derived by MISR over the Mediterranean. We integrate the data separately over the marine pixels of the western and eastern (Adriatic included) basins (Fig. 6).

2.3 Satellite OMI observations

The Ozone Monitoring Instrument (OMI) operating since October 2004 onboard of the EOS Aura satellite is a spectrometer with high spectral resolution (Levelt et al., 2006). OMI has a swath width of 2600 km and offers nearly global daily coverage with a spatial resolution for the UV-2 and VIS (UV-1) channels ranging from $13 \times 24(48)\ km^2$ at nadir. Here, we use data from the OMAERUV_v003 product containing retrievals from the OMI near-UV algorithm (Torres et al., 2007). The near-UV method of aerosol characterization uses remote-sensing measurements in two near-UV channels to detect aerosol absorption. This algorithm derives a variety of aerosol radiative properties, such as an aerosol index (AI), AOD, AAOD (uncertainty of ±(0.05 + 30 %)) and SSA (uncertainty of ±0.03) for clear-sky conditions. Here, we use SSA retrieved at 500 nm (Table 3) for the period 2004 to 2010 and we integrate over the same two Mediterranean sub-basins as with MISR (Fig. 6). In general, OMI near-UV aerosol AOD, AAOD and SSA retrievals

are more reliable over land than over water surfaces. The near-UV retrieval method is particularly sensitive to carbonaceous and mineral dust aerosols. The main source of uncertainty in the application of the near-UV technique to OMI observations is sub-pixel cloud contamination due to the large size of the OMI footprint. OMI measurements in the near-UV also depend on the height of the aerosol layer above the ground (Torres et al., 1998). Other possible sources of error include surface albedo effects and assumptions about particle size distribution and refractive index.

2.4 Satellite MODIS (Deep Blue) observations

The MODIS sensor is a 36-channel spectrometer (0.412–14.2 µm) with daily global coverage. The MODIS retrieval algorithm (hereafter referred as the MODIS standard algorithm) retrieves AOD over water and dark land surfaces, and fine-mode-fraction over water, at 10 km spatial resolution, aggregated to $1^\circ \times 1^\circ$ for the global level 3 product. The algorithm has two components, one applied over ocean (Tanré et al., 1997) and the other, based on the dark target approach, over land (Kaufman et al., 1997). In parallel with the aerosol retrievals classically conducted over the dark vegetation, the Deep Blue aerosol algorithm was developed to infer aerosol properties over highly reflective surfaces, using the blue channels radiance measurements (Hsu et al., 2004). When the retrieval algorithm successfully identifies the aerosols in the scene as "Fine or Mixed Aerosols", the corresponding values of AOD and Ångström exponent (AOD spectral dependence) are reported. For "dust-dominant" cases, SSA is retrieved (uncertainty of ±0.04 at 490 nm, see Hsu et al., 2004) over land surfaces at three different wavelengths (Table 3) in addition to AOD (uncertainty of (0.05 + 20 %, see Sayer et al., 2012) and the associated Ångström Exponent (AE). In this study, we used the monthly (MOD08_M3-level 3) SSA level-3 collection 5.1 product derived from Terra MODIS (http://ladsweb.nascom.nasa.gov/data/).

3 Results and discussions

3.1 Aerosol absorption optical depth

AAOD (level 2) has been derived from AERONET observations at different wavelengths. We first analyse AAOD at 440 nm obtained at the 22 selected AERONET sites (Fig. 1, Table 2). Over "pure" urban-industrialized regions (Table 2), AAOD falls between 0.027±0.01 and 0.05±0.01 with the maximum (0.047±0.010) observed at Rome (Table 2). In most cases, AAOD is around 0.03±0.01 for other urban-polluted sites. Long-term analysis of the AERONET records at the Modena and Rome sites, having around 10 yr of observations, does not reveal a clear AAOD tendency excepted over Rome, where a decrease is observed ($-0.0005\,yr^{-1}$) between 2001 and 2011 (Fig. 7). For periods of 3–5 yr between 2005 and 2008, Toulon and Thessaloniki display a possible decrease in AAOD (not shown), though the period of observations is too short to derive an AAOD tendency with confidence.

Mediterranean urban AAODs obtained at 440 nm are in the same magnitude range as those observed over other urban sites such as Creteil/Paris (∼0.015 ± 0.01) or Mexico (∼0.05 ± 0.01), but are generally higher than AAOD obtained at GSFC (AAOD < 0.010) or over other sites along the US Atlantic coast (AAOD ∼ 0.01 for the same wavelength) as reported by Russell et al. (2010). Compared to AAOD obtained during SAFARI (Southern Africa Regional Science Initiative) for smoke aerosols in southern Africa (AAOD ∼ 0.2 at 440 nm, see Russell et al., 2010) or in the Japan–Korea region during ACE-Asia for mixed particles (AAOD of about 0.1 at 440 nm), AAOD derived over the Mediterranean display lower values.

AERONET observations (Table 2) indicate that "dusty" sites (defined in Table 1) are logically characterized by larger mean AAOD (at 440 nm) from 0.037 ± 0.019 at Lampedusa to 0.055 ± 0.020 at Blida and 0.056 ± 0.041 at Oristano with values in the range 0.045–0.052 at Malaga, Granada, Nes Ziona and Sede Boker. Sites under desert dust influence seem to have experienced a decrease in AAOD (not shown) although conclusions made over such short time periods are highly uncertain (2003–2011 for Lampe-

dusa, 2004–2009 for Blida). This observed decrease is consistent with the results obtained by Zhang and Reid (2010), who showed a negative trend in AOD of −0.022 per decade using the ten-year (2000–2009) Data Assimilation quality MISR/MODIS combined aerosol product over ocean. Other Mediterranean sites under the influence of dust aerosols display significant AAOD ∼ 0.050. It should also be noted that similar values are found for AAOD observed over Puerto Rico during the PRIDE dust experiment (AAOD ∼ 0.05–0.06 at 440 nm) and over dusty sites in Bahrain/Persian Gulf, Solar Village/Saudi Arabia or Cape Verde (Russell et al., 2010). A linear correlation between AAOD and latitude (Fig. 3) is found significant (at the 0.01 level).

3.2 Aerosol Absorption Angström Exponent (AAE)

3.2.1 Aerosol level-2 product

As reported by Russell et al. (2010), the spectral dependence of AAOD, as defined in Eq. (1), can provide useful information on the contribution different aerosol types make to the shortwave absorption:

$$\mathrm{AAOD} = K\lambda^{-\mathrm{AAE}} \quad (2)$$

It follows that an AAE of 1.0 corresponds to λ^{-1} dependence of absorption. Due to its relatively constant refractive index, the absorption spectrum of fossil fuel Black Carbon (BC) aerosols is expected to exhibit AAE of about 1.0 (Sun et al., 2007). Laboratory studies and field measurements taken in urban areas support this statement (e.g. Bond and Bergstrom, 2006; Sciare et al., 2011). Following the BC nomenclature, Brown Carbon (BrC) is a recently introduced term for a class of light-absorbing carbonaceous material, which, unlike BC, has an imaginary part (k) of its refractive index that increases toward shorter visible and ultraviolet (UV) wavelengths, resulting in an AAE much larger than unity (Moosmüller et al., 2009). As described by Moosmüller et al. (2009), BrC is part of Organic Carbon (OC), with OC aerosols having previously been

assumed to absorb only weakly in the visible spectral region. Recent studies have suggested that the optical properties of BrC may be due to water-soluble organic carbon (WSOC) compounds and in particular, to humic-like substances (HULIS), which can have an AAE as large as 6–7 (Hoffer et al., 2006). The main sources of water-soluble BrC are biomass burning and, to a lesser extent, primary emissions from fossil fuel and secondary organic aerosols (Hecobian et al., 2010).

In addition to the chemical composition of aerosols, Gyawali et al. (2009) have shown recently that the AAE of BC cores (with diameter > 10 nm) that are coated by scattering shells may deviate from the typically assumed AAE of 1 relationship. Lack and Cappa (2010) have shown that BC cores coated by scattering shells can produce AAE values up to 1.6. This finding clearly complicates the attribution of observed AAE larger than 1 to BrC vs. mixing state. It should be also remembered that AAE is highly dependent of the wavelengths used in the calculation (Russel et al., 2010, Bahadur et al., 2012).

The mean and associated standard deviations of level 2 AAE obtained over AERONET sites are reported in Table 2 (AAE presented in this study is always calculated between 440 and 880 nm). Our results indicate that average AAE values obtained over the Mediterranean fall between 0.99 and 2.16. For the urban polluted sites (Lecce, Toulon, Rome, Thessaloniki, Messina, Barcelona, Burjassot and Athens), AAE is larger than 1, with a maximum of 1.5 in Rome (see Table 2). Such AAE values obtained over urban Mediterranean sites are similar to those obtained for other urban sites by Russell et al. (2010) (AAE ∼ 0.95, 1.40, 1.20, estimated between 440 and 880 nm for GSFC, Creteil/Paris and Mexico City, respectively). We note that AAE obtained at urban sites in the Eastern Mediterranean basin are generally higher than those reported by Russell et al. (2010).

As shown in Table 2 and Fig. 8a, Mediterranean dusty sites present larger AAE (∼ 1.96) compared to urban locations (∼ 1.31). Lampedusa and Blida are characterized by slightly different averaged AAE (and associated standard deviation) of 2.16 (± 0.67) and 1.80 (± 0.42), respectively, which could be due to differences in dust size distribution. Indeed, a higher contribution of coarse dust particles near the sources (Blida)

could lead to larger AAOD at 880 nm decreasing AAE compared to sites far from the dust sources (Lampedusa). Compared to reference values, Mediterranean dust AAE values are found to be slightly lower than observed during the PRIDE (dust aerosols) or ACE-Asia (mixed dust-urban-industrial particles) experiments (AAE ~ 2.34 and 2.27, respectively). However, Mediterranean dust AAE values are similar to those observed over Bahrain/Persian Gulf (2.10, calculated between 440 and 870 nm) and Arabia (1.80, between 440 and 870 nm). Finally, dust AAE obtained over the Mediterranean are found to be consistent with AAE observed over Western Africa at Banizoumbou (1.7 ± 0.6, estimated between 440 and 870 nm), Dakar (1.9 ± 0.6) and Ougadougou (1.6 ± 0.5) as reported by Giles et al. (2012).

One important result concerns the AAE regional gradient which appears over the Mediterranean. Analysis of AERONET level 2 data (excluding AERONET sites affected by the presence of dust, such as Blida and Lampedusa) display lower mean AAE values over the Western basin (Table 2 and Fig. 8b). Calculated AAE over Spain (including Burjassot, Granada and Barcelona) and France (Toulon, Villefranche sur Mer and Ersa) are between 0.99 and 1.22 (Table 2) and clearly increase over Italy, Greece (Thessaloniki and Athens) and Crete Island, with AAE values comprised between 1.30 and 1.70. Average AAE for Eastern and Western AERONET sites are about 1.39 and 1.33, respectively (Fig. 8b). This AAE regional gradient indicates that mineral dust and/or organic absorbing particles might make a larger contribution to the total aerosol load over the Eastern Mediterranean. As the AERONET level-2 product retains only high-quality cases having AOD higher than 0.4 at 440 nm for estimating AAOD, this gradient supports a larger influence of mineral dust over the Eastern region. Figure 9 plots the particle size distribution retrieved from level-2 AERONET sky measurements (Dubovik et al., 2000) and averaged over the eastern and western stations. Larger concentrations are generally found in the eastern basin but the difference appears only significant for the coarse mode. If we fit those distributions by a bimodal lognormal distribution, the coarse mode is found to have a slightly larger relative contribution in the eastern basin (Table 4). In addition, Fig. 10 reports AAE for northern and southern AERONET sites

classified for the western (Fig. 10a) and eastern (Fig. 10b) basins. In this case, the regional latitudinal gradient is clearly more pronounced over the western basin, where the mean AAE is about 1.77 and 1.22 for the northern and southern AERONET sites, respectively, due to the desert dust influence. This gradient is also well observed over the eastern basin with a moderate difference in AAE between the southern (mean AAE of 1.47) and northern (mean AAE of 1.34) AERONET sites, respectively.

3.2.2 Aerosol level 1.5 product

As mentioned below, AERONET data quality criteria do not support the study of the brown carbon influence on absorbing properties in most cases, as smoke plumes are generally characterized by moderate AOD ($0.2 < \text{AOD} < 0.5$). However and as already mentioned, smoke aerosols that contain high concentrations of organics are characterized by large AAE (for SAFARI African biomass smoke, AAE ~ 1.45, calculated between 325 and 1000 nm; Russell et al., 2010). In order to investigate the possible role of smoke aerosols, we have conducted complementary analyses using AERONET level-1.5 retrievals with data screened for Angström Exponent > 1.0 to avoid mineral dust aerosols. For these data (AOD > 0.2 and AE > 1.0), AAOD uncertainties are about 0.01 (O. Dubovik, personal communication, 2013). Results of calculations are shown in Fig. 11 for two different AERONET sites: Crete and Rome (Barcelona and Lecce are provided in annexe material), demonstrating that AAE values larger than 1 are derived in a number of cases. Over Rome, we observe AAE values reaching 1.6–1.7 in number of cases (mean of 1.19), suggesting that organic particles could affect shortwave absorption over this site. Similar conclusions are obtained in Lecce and Athens (not shown), with average AAE of 1.15. In Lecce, AAE values larger than 1 are observed in all years from 2003 to 2011 with maxima during summer (not shown), indicating that a significant fraction of the aerosol absorption in Southern Italy is due to BrC. However, the Forth Crete site is characterized by lower mean AAE (1.05) even though values up to 1.7 were derived during summer 2003 intense heat wave event. These higher values are consistent with a large agriculture waste biomass burning smoke contribution orig-

inating from the region surrounding the Black Sea and transported over Crete (Sciare et al., 2003, 2008). This influence of wood burning shows a maximum during summertime, consistent with the maxima in AAOD observed in that season over Moldova and Northern Greece, which are on the path of air masses originating from the Black Sea region and transported over the Eastern Mediterranean. Finally, over Barcelona, even if the mean value is near unity, indicating that BC aerosol is the main contributor to absorption, a large range of AAE is also observed, with maxima around 1.6. Further analysis is needed to link the calculated AAE with the chemical composition of aerosols over different AERONET sites when such data are available. To conclude, such additional analysis of AERONET level 1.5 data reveal that, in addition to dust particles, organic aerosols also contribute to shortwave absorption over the Mediterranean. This result demonstrates that current regional climate models treating OC as nonabsorbing over Mediterranean underestimate the total warming effect of carbonaceous particles by neglecting part of atmospheric heating.

3.3 Aerosol Single Scattering Albedo (SSA)

3.3.1 AERONET level 2 observations

As mentioned previously, SSA (level-2) has been determined from AERONET inversions at different wavelengths. Long-term SSA observations (more than 5 yr, i.e. Modena and Rome) display average daily values between 0.70 ± 0.04 and 0.97 ± 0.04 (440 nm) with no significant trends. Over urban sites, Table 2 indicates that in most cases Mediterranean urban-industrial polluted locations appear as "moderately" absorbing with SSA close to $\sim 0.95 \pm 0.04$ (at 440 nm). Such SSA values are found to be in the same range as AERONET SSA observed in Creteil (a suburb of Paris) $\sim 0.94 \pm 0.04$ (at 440 nm) and lower than SSA obtained at GFSC (Goddard Space Flight Center Greenbelt, Maryland) (0.98 ± 0.04 at 440 nm) (Dubovik et al., 2002). Over the Mediterranean, the highest urban-industrial aerosol absorption is observed for Rome (SSA of 0.89) and Athens (0.90) in accordance with AAOD observations. It should be noted that

such values are in the same range as the one derived in Mexico (SSA $\sim$ 0.90; Dubovik et al., 2002). The observed wide SSA variability for Mediterranean urban locations can probably be explained by differences in emissions, environmental and meteorological conditions.

Even if not directly comparable with in-situ SSA observations due to differences in temporal sampling and vertical integration, we attempted to compare AERONET SSA with in-situ estimates for urban/industrial Mediterranean zones. Over Southern France, AERONET SSA is comparable to in-situ observations published by Saha et al. (2008) and Mallet et al. (2003, 2004), with SSA of 0.85 (here at 550 nm). Similar concurrence is observed with SSA aircraft measurements obtained by Mallet et al. (2005) over the Marseille/Etang de Berre area (SSA $\sim$ 0.88–0.93, at 550 nm).

Over Southern Spain, AERONET SSA (Burjassot and Granada) display mean values of 0.93 ± 0.04 and 0.90 ± 0.04 (at 440 nm), consistent with the values reported by Horvarth et al. (2002) at Almeria (SSA of 0.86–0.90). Over Greece, the differences between AERONET (0.91 ± 0.04 at Athens and 0.94 ± 0.04 at Thessaloniki) and in-situ observations (0.82 in Thessaloniki, Chazette and Liousse, 2001) are more pronounced. Over south-eastern Italy, Tafuro et al. (2007) reported a value of $\sim$0.94 during summer for anthropogenic particles, consistent with Lecce and Messina AERONET measurements (0.92 ± 0.04 and 0.94 ± 0.04).

For "dusty" sites, average SSA is in the range of $0.90–0.92 \pm 0.04$ at 440 nm (see Table 2) indicating that dust particles are moderately absorbing over the Mediterranean. For this aerosol type, comparisons between AERONET SSA and in-situ observations are more limited, as most of estimates were obtained with remote-sensing techniques (Di Biagio et al., 2009; Meloni et al., 2004, 2008). In contrast to such "moderate" dust SSAs, several studies reported larger absorbing efficiencies over the Mediterranean. Di Biagio et al. (2009) indicated that SSA (at 415.6 nm) for desert dust showed large variability, between 0.7 and 0.9 during the 2004 to 2007 period. Di Biagio et al. (2009) determined that 57 % of the dust events with SSA (at 415.6 nm) lower than 0.75 correspond to trajectories (at 750 m) originating from central Europe, and trajectories end-

ing at 2000 and 4000 m coming from Africa. In these cases, the presence of polluted absorbing particles at lower atmospheric levels explains the low SSA values. More recently, in the case of dust aerosols transported over Barcelona, Sicard et al. (2012) indicate surprisingly low dust SSA (~ 0.70 at 440 nm) due to the mixing of dust with smoke-polluted particles.

3.3.2 SSA spectral dependence

The SSA wavelength dependence obtained for urban and dusty AERONET sites is reported in Fig. 12a. We clearly note two opposite behaviours, an increase and a decrease of SSA with wavelengths, associated with dust and urban aerosol, respectively, and similar to that reported by Russell et al. (2010). Here, the SSA spectra for AERONET locations dominated by desert dust increase from ~ 0.90–0.92 ± 0.04 (at 440 nm) to ~ 0.95–0.96 ± 0.04 (at 1020 nm). In contrast, SSA is clearly decreasing for locations dominated by fine pollution aerosols, from ~ 0.92–0.93 ± 0.04 (at 440 nm) to ~ 0.91–0.92 ± 0.04 (at 1020 nm). Such a decrease seems less marked than those reported by Russell et al. (2010) for other anthropogenic sites.

Figure 12b presents the average SSA spectra obtained for the western and eastern Mediterranean AERONET sites. The mean value calculated at 440 nm for the eastern Mediterranean sites is slightly lower (~0.92 ± 0.04) than that over the western part (~0.94 ± 0.04). This result is consistent with AAE observations, suggesting a more pronounced contribution of dust particles over the Eastern basin. As shown in Fig. 12b, this finding is based only on the shortest wavelengths provided by AERONET (440 nm). Indeed, the difference in SSA becomes negligible for longer wavelengths (670, 870 and 1020 nm, Fig. 12b). In that sense, new AERONET photometer retrievals at 340 nm should be very helpful, but unfortunately are not yet available. Also, as shown in Fig. 12b, the SSA spectra for western AERONET sites decrease with increasing wavelengths, from 0.94 ± 0.04 (440 nm) to 0.92 ± 0.04 (1020 nm), unlike the Eastern sites, where SSA increases between 440 and 670 nm, which is a signature of dust particles (Dubovik et al., 2002).

3.3.3 SSA satellite observations

Figures 13 and 14 present SSA observations for each sensor: OMI (500 nm), MISR (558 nm) and MODIS Deep Blue (DB) (470 nm) averaged for the summer (JJA) and spring (MAM) seasons, respectively. As shown in Fig. 13 and detailed in Table 3, MODIS DB derives SSA only over bright surfaces (see Hsu et al., 2004; Wells et al., 2012).

Concerning the OMI sensor, we observe a clear North–South gradient with lower values over the Southern Mediterranean and higher SSA (~ 1 at 550 nm) over a large part of the European continent. Note that a region of lower SSA (~ 0.85–0.90 at 550 nm) occurs, especially over Morocco and the Algerian coast. This result is consistent with recent findings presented by Valenzuela et al. (2012), who showed that particles have marked absorbing properties during dust events, corresponding to air masses transported from North Morocco and northwest Algeria. This "absorbing" zone (Fig. 13) is also identified by MODIS DB but with a larger regional extent compared to OMI. Indeed, MODIS DB indicates SSA between 0.90 and 0.95 over Northern Africa, South of Turkey and Spain. Compared to OMI and MISR, Northern Africa appears "more absorbing" based on the MODIS DB product, but it should be remembered that the retrieval wavelengths are different among the three sensors (especially between MODIS and MISR), which could explain in part the lower values obtained from MODIS DB (ΔSSA is around 0.03 between 470 and 550 nm, Dubovik et al., 2002).

As mentioned below, when using MODIS DB data, a large part of Algeria (25–30° N, 0–10° E), Tunisia and western Libya are characterized by SSA ~ 0.90. This regional pattern is consistent with some identified dust sources reported by Laurent et al. (2008). The Eastern part of Libya (25–28° N, 10–15° E) also produces significant concentrations of mineral dust and is also correlated with moderate SSA. For these specific regions, a large concentration of coarse dust aerosols could reduce the total bulk dust SSA as shown by McConnell et al. (2008).

Concerning MISR, we observe near unity SSAs (555 nm) during JJA over a large part of the African continent with some lower values (~ 0.95) derived over Morocco, North Algeria and Tunisia, but the contrast is less marked than for the OMI and MODIS observations. Over Africa, MISR SSA is clearly higher (+0.1) than OMI. As reported by Kahn et al. (2010), MISR tends to obtain SSAs at or near unity, especially when the AOD is too low to produce good SSA constraints. Kahn et al. (2010) indicate that information about particle properties in the MISR data decreases significantly when the total column visible AOD is below 0.15 or 0.2 (at 5[illegible]m), and in such cases, should not be used for quantitative analysis according to the MISR Data Quality Statement distributed with the aerosol products. Aerosol [illegible] information content also diminishes as AOD decreases below certain values for a[illegible]mote sensing techniques (this effect is not as well documented for MODIS and OMI). Over the Mediterranean Sea, MISR derives lower SSA (~ 0.92–0.96) compared to land surfaces, associated with a north-south gradient. One can clearly note specific regions with lo[illegible]SA (~ 0.85–0.90) over the Aegean, Adriatic and Black Seas, possibly due to the p[illegible]nce of anthropogenic absorbing particles.

For the spring period (Fig. 14), Southern Europe (Italy, Greece, Turkey and Spain) appears to be less absorbing than during summer, with ΔSSA (spring minus summer SSA) of +0.025. The increase could be due to a lower concentration of polluted absorbing aerosols during spring compared to summer. In contrast, a large part of Northern Africa appears as more absorbing ($-0.01 < \Delta SSA < -0.02$) during spring compared to summer, with a maximum over the eastern part (Libya). This may due to higher emissions of dust during spring. This result is consistent with MODIS DB data, which shows a decrease of about −0.02 of SSA over Northern Africa during spring. MISR produces different results over Southern continental Europe, with higher SSA during summer compared to spring (ΔSSA ~ +0.01). Similar increases in SSA during summer are also detected over the Mediterranean coastal zones of Algeria and Morocco. Over the Sea (especially for the Oriental basin), we obtain consistent results, with lower SSA during

the summer, certa[illegible]y due to the accumulation of absorbing polluted particles at this time.

Finally, at regional scales, MISR displays a nearly constant SSA (~ 0.97–0.98) over the Mediterranean Sea during summer and spring as well as OMI (Fig. 15). Unlike OMI, the SSA geographical gradient observed using AERONET data is better captured by MISR, amounting to lower SSA over the eastern basin (~ 0.96–0.97) compared to the western one (~ 0.98–0.99), especially during summer, when polluted particles are present. The uncertainty associated with MISR SSA (see Sect. 2.2 above) retrievals does not allow distinguishing different absorbing properties for the two basins during spring (Fig. 15). Due to the uncertainty associated with the OMI SSA product, no conclusion about the differences in absorbing properties between the Eastern and Western basins can be drawn from OMI data (Fig. 15).

4 Conclusions

A multi-year climatology of column-effective aerosol absorption properties obtained over the Mediterranean from AERONET ground-based and satellite (MISR, OMI, MODIS Deep Blue) remote sensing observations is presented. The focus of this study was on characterizing Aerosol Absorption Optical Depth (AAOD) and Single Scattering Albedo (SSA), and their spectral dependence. The AAOD data set is composed of daily averaged AERONET level 2 data from 22 stations mainly under the influence of urban-industrial and/or soil dust aerosols. The data sets span 1996–2012, but most data are from the 2003–2011 period. The SSA data set includes both AERONET and satellite products. Since AERONET level 2 absorption products are limited to high aerosol load (AOD at 440 nm > 0.4), which are most often related to the presence of desert dust, we also considered level 1.5 AAOD data despite their higher uncertainty. Satellite-derived SSA data are monthly level 3 products mapped at the regional scale, and we focus on the spring and summer seasons of maximum aerosol load in the Mediterranean. Satellite products include (i) the 0.5° × 0.5° product from Terra/MISR over 2000–2011,

(ii) the 48 km × 48 km product from OMI near-UV algorithm over 2004–2010, and (iii) the 1° × 1° product from Terra/MODIS Deep-Blue algorithm over 2005–2011, derived only over land in dusty conditions.

AAOD values obtained from sun-photometer observations over the Mediterranean at 440 nm ranged from 0.024 ± 0.010 to 0.050 ± 0.010 for urban sites (with maxima observed over Rome), whereas for dusty sites, AAOD varied from 0.040 ± 0.010 to 0.055 ± 0.010. The analysis of the corresponding SSA values showed that aerosol over Mediterranean urban-industrial locations appeared "moderately" absorbing, with SSA at 440 nm close to ~ 0.94–0.95 ± 0.04, although in some locations the aerosol was as absorbing as heavily polluted sites such as Mexico City.

The spectral dependence of absorbing properties was also studied, using the Absorbing Angström Exponent (AAE) estimated between 440 and 870 nm. For most Mediterranean sites, AAE is larger than 1, indicating strong shortwave absorption that can be associated with the presence of Brown Carbon (BrC) and/or mineral dust (having high iron content) aerosols. Sun-photometer level-2 data analysis indicates a moderate AAE regional gradient, with higher values obtained over the eastern basin ($AAE_{East.}$ = 1.39/$AAE_{West.}$ = 1.33), mainly due to the presence of mineral dust particles. In parallel, the North–South AAE gradient is more pronounced, especially over the western basin, with AAE_{North} and AAE_{South} of about 1.22 and 1.77, respectively.

The complementary analysis using level 1.5 AERONET retrievals with data screened to avoid mineral dust aerosols (i.e., AOD > 0.2 and Angström Exponent > 1.0) show that some Mediterranean sites are affected by organic absorbing aerosols (mean AAE ~ 1.15), especially Rome, Lecce, Burjassot and Athens. The effect is found to be lower for the Barcelona and Forth Crete AERONET sites (mean AAE of about 1.0). This result highlights that current regional climate models that treat OC as purely scattering over the Mediterranean underestimate the total warming effect of carbonaceous aerosols and neglect part of the atmospheric heating due to particles.

In addition, we explored the possibility of using satellite products for characterising the spatial distribution of aerosol absorption over the Mediterranean. Our results suggest that columnar values of aerosol SSA obtained from OMI, MISR and MODIS DB reveal significant differences. OMI and MODIS detect an absorbing zone over Northeast Africa with SSA ~ 0.90 (at 470–500 nm), which is not detected by MISR. In a contrast, MISR seems able to capture the East–West SSA gradient during summer, as observed from AERONET; however the satellite retrievals provide only qualitative constraints on SSA. In addition, the analysis of satellite SSA indicates that the Mediterranean aerosol appears more absorbing during summer compared to spring, which could be due to a larger proportion of sunlight-absorbing particles, such as desert dust and smoke.

Acknowledgements. This work was undertaken is the framework of the MISTRALS/ChArMEx programme. We acknowledge the AERONET and PHOTONS sun-photometer networks and the PIs of the 22 selected stations and their staff for their work to produce the dataset used in this study. We acknowledge the OMI PIs for providing satellite observations.

The publication of this article is financed by CNRS-INSU.

References

Antoine, D. and Nobileau, D.: Recent increase of Saharan dust transport over the Mediterranean Sea, as revealed from ocean color satellite (SeaWiFS) observations, J. Geophys. Res., 111, D12214, doi:10.1029/2005JD006795, 2006.

Bahadur, R., Praveen, P. S., Yangyang, X., and Ramanathan, V.: Solar absorption by elemental and brown carbon determined from spectral observations, Proc. Natl. Acad. Sci. USA, 109, 17366–17371, doi:10.1073/pnas.1205910109, 2012.

Barnaba, F. and Gobbi, G. P.: Aerosol seasonal variability over the Mediterranean region and relative impact of maritime, continental and Saharan dust particles over the basin from MODIS data in the year 2001, Atmos. Chem. Phys., 4, 2367–2391, doi:10.5194/acp-4-2367-2004, 2004.

Bond, T. C. and Bergstrom, R. W.: Light absorption by carbonaceous particles: an investigative review, Aerosol Sci. Technol., 40, 27–47, 2006.

Chazette, P. and Liousse, C.: A case study of optical and chemical ground apportionment for urban aerosols in Thessaloniki, Atmos. Environ., 35, 2497–2506, 2001.

Di Biagio, C., di Sarra, A., Meloni, D., Monteleone, F., Piacentino, S., and Sferlazzo, D.: Measurements of Mediterranean aerosol radiative forcing and influence of the single scattering albedo, J. Geophys. Res., 114, D06211, doi:10.1029/2008JD011037, 2009.

Dubovik, O. and King, M. D.: A flexible inversion algorithm for retrieval of aerosol optical properties from Sun and sky radiance measurements, J. Geophys. Res., 105, 20673–20696, 2000.

Dubovik, O., Holben, B. N., Eck, T. F., Smirnov, A., Kaufman, Y. J., King, M. D., Tanré, D., and Slutsker, I.: Variability of absorption and optical properties of key aerosol types observed in worldwide locations, J. Atmos. Sci., 59, 590–608, 2002.

Dubovik, O., Sinyuk, A., Lapyonok, T., Holben, B. N., Mishchenko, M., Yang, P., Eck, T. F., Volten, H., Munoz, O., Veihelmann, B., van der Zande, W. J., Leon, J.-F., Sorokin, M., and Slutsker, I.: Application of spheroid models to account for aerosol particle nonsphericity in remote sensing of desert dust, J. Geophys. Res., 111, D11208, doi:10.1029/2005JD006619, 2006.

Dubovik, O., Herman, M., Holdak, A., Lapyonok, T., Tanré, D., Deuzé, J. L., Ducos, F., Sinyuk, A., and Lopatin, A.: Statistically optimized inversion algorithm for enhanced retrieval of aerosol properties from spectral multi-angle polarimetric satellite observations, Atmos. Meas. Tech., 4, 975–1018, doi:10.5194/amt-4-975-2011, 2011.

Foltz, G. R. and McPhaden, M. J.: Impact of Saharan dust on tropical North Atlantic SST, J. Climate, 21, 5048–5060, 2008.

Formenti, P., Boucher, O., Reiner, T., Sprung, D., Andreae, M. O., Wendisch, M., Wex, H., Kindred, D., Dewey, K., Kent, J., Tzortziou, M., Vasaras, A., and Zerefos, C.: STAAARTE-MED 1998 summer airborne measurements over the Aegean Sea, 1. Aerosol particles and trace gases, J. Geophys. Res., 107, 4450, doi:10.1029/2001JD001337, 2002a.

Formenti, P., Boucher, O., Reiner, T., Sprung, D., Andreae, M. O., Wendisch, M., Wex, H., Kindred, D., Tzortziou, M., Vasaras, A., and Zerefos, C.: STAAARTE-MED 1998 summer airborne measurements over the Aegean Sea, 2. Aerosol scattering and absorption, and radiative calculations, J. Geophys. Res., 107, 4451, doi:10.1029/2001JD001536, 2002b.

Fotiadi, A., Hatzianastassiou, N., Drakakis, E., Matsoukas, C., Pavlakis, K. G., Hatzidimitriou, D., Gerasopoulos, E., Mihalopoulos, N., and Vardavas, I.: Aerosol physical and optical properties in the Eastern Mediterranean Basin, Crete, from Aerosol Robotic Network data, Atmos. Chem. Phys., 6, 5399–5413, doi:10.5194/acp-6-5399-2006, 2006.

Gerasopoulos, E., Andreae, M. O., Zerefos, C. S., Andreae, T. W., Balis, D., Formenti, P., Merlet, P., Amiridis, V., and Papastefanou, C.: Climatological aspects of aerosol optical properties in Northern Greece, Atmos. Chem. Phys., 3, 2025–2041, doi:10.5194/acp-3-2025-2003, 2003.

Giles, D. M., Holben, B. N., Eck, T. F., Sinyuk, A., Smirnov, A., Slutsker, I., Dickerson, R. R., Thompson, A. M., and Schafer, J. S.: An analysis of AERONET aerosol absorption properties and classifications representative of aerosol source regions, J. Geophys. Res., 117, D17203, doi:10.1029/2012JD018127, 2012.

Giorgi, F.: Climate change hot-spots, Geophys. Res. Lett., 33, L08707, doi:10.1029/2006GL025734, 2006.

Giorgi, F. and Lionello, P.: Climate change projections for the Mediterranean region, Global Planet. Change, 63, 90–104, 2008.

Gyawali, M., Arnott, W. P., Lewis, K., and Moosmüller, H.: In situ aerosol optics in Reno, NV, USA during and after the summer 2008 California wildfires and the influence of absorbing and non-absorbing organic coatings on spectral light absorption, Atmos. Chem. Phys., 9, 8007–8015, doi:10.5194/acp-9-8007-2009, 2009.

Hatzianastassiou, N., Gkikas, A., Mihalopoulos, N., Torres, O., and Katsoulis, B. D.: Natural versus anthropogenic aerosols in the eastern Mediterranean basin derived from multiyear TOMS and MODIS satellite data, J. Geophys. Res., 114, D24202, doi:10.1029/2009JD011982, 2009.

Holben, B. N., Eck, T. F., Slutsker, I., Tanré, D., Buis, J. P., Setzer, A., Vermote, E., Reagan, J. A., Kaufman, Y., Nakajima, T., Lavenu, F., Jankowiak, I., and Smirnov, A.: AERONET – A federated instrument network and data archive for aerosol characterization, Remote Sens. Environ., 66, 1–16, 1998.

Hecobian, A., Zhang, X., Zheng, M., Frank, N., Edgerton, E. S., and Weber, R. J.: Water-Soluble Organic Aerosol material and the light-absorption characteristics of aqueous extracts measured over the Southeastern United States, Atmos. Chem. Phys., 10, 5965–5977, doi:10.5194/acp-10-5965-2010, 2010.

Hoffer, A., Gelencsér, A., Guyon, P., Kiss, G., Schmid, O., Frank, G. P., Artaxo, P., and Andreae, M. O.: Optical properties of humic-like substances (HULIS) in biomass-burning aerosols, Atmos. Chem. Phys., 6, 3563–3570, doi:10.5194/acp-6-3563-2006, 2006.

Horvath, H., Alados Arboledas, L., Olmo, F. J., Jovanovic, O., Gangl, M., Sanchez, C., Sauerzopf, H., and Seidl, S.: Optical characteristics of the aerosol in Spain and Austria and its effect on radiative forcing, J. Geophys. Res., 107, 4386, doi:10.1029/2001JD001472, 2002.

Hsu, C. N., Tsay, S.-C., and King, M. D.: Aerosol properties over bright-reflecting source regions, IEEE T. Geosci. Remote, 42, 557–569, doi:10.1109/TGRS.2004.824067, 2004.

Kahn, R., Petzold, A., Wendisch, M., Bierwirth, E., Dinter, T., Esselbörn, M., Fiebig, M., Heese, B., Knippertz, P., Muller, D., Schladitz, A., and von Hoyningen-Huene, W.: Desert dust aerosol air mass mapping in the western Sahara, using particle properties derived from space-based multi-angle imaging, Tellus B, 61, 239–251, doi:10.1111/j.1600-0889.2008.00398.x, 2009.

Kahn, R. A., Gaitley, B. J., Garay, M. J., Diner, D. J., Eck, T. F., Smirnov, A., and Holben, B. N.: Multiangle Imaging SpectroRadiometer global aerosol product assessment by comparison with the Aerosol Robotic Network, J. Geophys. Res., 115, D23209, doi:10.1029/2010JD014601, 2010.

Kaufman, Y. J., Tanré, D., Remer, L. A., Vermote, E. F., Chu, A., and Holben, B. N.: Operational remote sensing of tropospheric aerosol over land from EOS moderate resolution imaging spectroradiometer, J. Geophys. Res., 102, 17051–17067, 1997.

Kubilay, N., Cokacar, T., and Oguz, T.: Optical properties of mineral dust outbreaks over the northeastern Mediterranean, J. Geophys. Res., 108, 4666, doi:10.1029/2003JD003798, 2003.

Lack, D. A. and Cappa, C. D.: Impact of brown and clear carbon on light absorption enhancement, single scatter albedo and absorption wavelength dependence of black carbon, Atmos. Chem. Phys., 10, 4207–4220, doi:10.5194/acp-10-4207-2010, 2010.

Lau, K. M., Kim, K. M., Sud, Y. C., and Walker, G. K.: A GCM study of the response of the atmospheric water cycle of West Africa and the Atlantic to Saharan dust radiative forcing, Ann. Geophys., 27, 4023–4037, doi:10.5194/angeo-27-4023-2009, 2009.

Laurent, B., Marticorena, B., Bergametti, G., Léon, J.-F., and Mahowald, N.: Modeling mineral dust emissions from the Sahara desert using new surface properties and soil database, J. Geophys. Res., 113, D14218, doi:10.1029/2007JD009484, 2008.

Levelt, P. F., Hilsenrath, E., Leppelmeier, G. W., van den Oord, G. H. J., Bhartia, P. K., Tamminen, J., de Haan, J. F., and Veefkind, J. P.: Science objectives of the Ozone Monitoring Instrument, IEEE T. Geosci. Remote Sens., 44, 1199–1208, doi:10.1109/TGRS.2006.872336, 2006.

Lionello, P., Abrantes, F., Congedi, L., Dulac, F., Gacic, M., Gomis, D., Goodess, C., Hoff, H., Kutiel, H., Luterbacher, J., Planton, S., Reale, M., Schröder, K., Struglia, M. V., Toreti, A., Tsimplis, M., Ulbrich, U., and Xoplaki, E., (Introduction): Mediterranean climate: background information, in: The Climate of the Mediterranean Region: From the Past to the Future, edited by: Lionello, P., Elsevier, 590 pp., 2012.

Mallet, M., Roger, J. C., Despiau, S., Dubovik, O., and Putaud, J. P.: Microphysical and optical properties of aerosol particles in urban zone during ESCOMPTE, Atmos. Res., 69, 73–97, 2003.

Mallet, M., Roger, J. C., Despiau, S., Putaud, J. P., and Dubovik, O.: A study of the mixing state of black carbon in urban zone, J. Geophys. Res., 109, D04202, doi:10.1029/2003JD003940, 2004.

Mallet, M., Van Dingenen, R., Roger, J. C., Despiau, S., and Cachier, H.: In situ airborne measurements of aerosol optical properties during photochemical pollution events, J. Geophys. Res., 110, D03205, doi:10.1029/2004JD005139, 2005.

Mallet, M., Pont, V., Liousse, C., Roger, J. C., and Dubuisson, P.: Simulation of aerosol radiative properties with the ORISAM-RAD model during a pollution event (ESCOMPTE 2001), Atmos. Environ., 40, 7696–7705, 2006.

Mallet, M., Tulet, P., Serça, D., Solmon, F., Dubovik, O., Pelon, J., Pont, V., and Thouron, O.: Impact of dust aerosols on the radiative budget, surface heat fluxes, heating rate profiles and convective activity over West Africa during March 2006, Atmos. Chem. Phys., 9, 7143–7160, doi:10.5194/acp-9-7143-2009, 2009.

Markowicz, K. M., Flatau, P. J., Ramana, M. V., Crutzen, P. J., and Ramanathan, V.: Absorbing mediterranean aerosols lead to a large reduction in the solar radiation at the surface, Geophys. Res. Lett., 29, 1968, doi:10.1029/2002GL015767, 2002.

Martonchik, J. V., Kahn, R. A., and Diner, D. J.: Retrieval of aerosol properties over land using MISR observations, in: Satellite Aerosol Remote Sensing Over Land, edited by: Kokhanovsky, A., Springer, Berlin, Germany, 2009.

McConnell, C. L., Highwood, E. J., Coe, H., Formenti, P. Anderson, B., Osborne, S., Nava, S., Desboeufs, K., Chen, G., and Harrison, M. A. J.: Seasonal variations of the physical and optical characteristics of Saharan dust: results from the Dust Outflow and Deposition to the Ocean (DODO) experiment, J. Geophys. Res., 113, D14S05, doi:10.1029/2007JD009606, 2008.

Meloni, D., Di Sarra, A., Di Iorio, T., and Fiocco, G.: Direct radiative forcing of Saharan dust in the Mediterranean from measurements at Lampedusa Island and MISR space-borne observations, J. Geophys. Res., 109, D08206, doi:10.1029/2003JD003960, 2004.

Meloni, D., di Sarra, A., Pace, G., and Monteleone, F.: Aerosol optical properties at Lampedusa (Central Mediterranean). 2. Determination of single scattering albedo at two wavelengths for different aerosol types, Atmos. Chem. Phys., 6, 715–727, doi:10.5194/acp-6-715-2006, 2006.

Meloni, D., di Sarra, A., Biavati, G., DeLuisi, J. J., Monteleone, F., Pace, G., Piacentino, S., and Sferlazzo, D. M.: Seasonal behavior of Saharan dust events at the Mediterranean island of Lampedusa in the period 1999–2005, Atmos. Environ., 41, 3041–3056, 2007.

Moosmüller, H., Chakrabarty, R. K., and Arnott, W. P.: Aerosol light absorption and its measurement: a review, J. Quant. Spectrosc. Rad. T., 110, 844–878, 2009.

Moulin, C., Lambert, C. E., Dayan, U., Masson, V., Ramonet, M., Bousquet, P., Legrand, M., Balkanski, Y. J., Guelle, W., Marticorena, B., Bergametti, G., and Dulac, F.: Satellite climatology of African dust transport in the Mediterranean atmosphere, J. Geophys. Res., 103, 13137–13144, 1998.

Nabat, P., Somot, S., Mallet, M., Chiapello, I., Morcrette, J. J., Solmon, F., Szopa, S., and Dulac, F.: A 4-D climatology (1979–2009) of the monthly aerosol optical depth distribution over the Mediterranean region from a comparative evaluation and blending of remote sensing and model products, Atmos. Meas. Tech. Discuss., 5, 8469–8538, doi:10.5194/amtd-5-8469-2012, 2012.

Pace, G., di Sarra, A., Meloni, D., Piacentino, S., and Chamard, P.: Aerosol optical properties at Lampedusa (Central Mediterranean). 1. Influence of transport and identification of different aerosol types, Atmos. Chem. Phys., 6, 697–713, doi:10.5194/acp-6-697-2006, 2006.

Papadimas, C. D., Hatzianastassiou, N., Mihalopoulos, N., Querol, X., and Vardavas, I.: Spatial and temporal variability in aerosol properties over the Mediterranean basin based on 6-year (2000–2006) MODIS data, J. Geophys. Res., 113, D11205, doi:10.1029/2007JD009189, 2008.

Papadimas, C. D., Hatzianastassiou, N., Mihalopoulos, N., Kanakidou, M., Katsoulis, B. D., and Vardavas, I.: Assessment of the MODIS Collections C005 and C004 aerosol optical depth products over the Mediterranean basin, Atmos. Chem. Phys., 9, 2987–2999, doi:10.5194/acp-9-2987-2009, 2009.

Ramanathan, V., Crutzen, P. J., Kiehl, J. T., and Rosenfeld, D.: Aerosols, climate, and the hydrological cycle, Science, 294, 2119–2124, 2001a.

Ramanathan, V., Crutzen, P. J., Lelieveld, J., Mitra, A. P., Althausen, D., Anderson, J., Andreae, M. O., Cantrell, W., Cass, G. R., Chung, C. E., Clarke, A. D., Coakley, J. A., Collins, W. D., Conant, W. C., Dulac, F., Heintzenberg, J., Heymsfield, A. J., Holben, B., Howell, S., Hudson, J., Jayaraman, A., Kiehl, J. T., Krishnamurti, T. N., Lubin, D., McFarquhar, G., Novakov, T., Ogren, J. A., Podgorny, I. A., Prather, K., Priestley, K., Prospero, J. M., Quinn, P. K., Rajeev, K., Rasch, P., Rupert, S., Sadourny, R., Satheesh, S. K., Shaw, G. E., Sheridan, P., and Valero, F. P. J.: The Indian Ocean Experiment: an integrated assessment of the climate forcing and effects of the Great Indo-Asian Haze, J. Geophys. Res. Atmos., 106, 28371–28399, 2001b.

Roger, J. C., Mallet, M., Dubuisson, P., Cachier, H., Vermote, E., Dubovik, O., and Despiau, S.: A synergetic approach for estimating the local direct aerosol forcing: application to an urban zone during the Expérience sur Site pour Contraindre les Modèles de Pollution et de Transport d'Emission (ESCOMPTE) experiment, J. Geophys. Res., 111, D13208, doi:10.1029/2005JD006361, 2006.

Russell, P. B., Bergstrom, R. W., Shinozuka, Y., Clarke, A. D., DeCarlo, P. F., Jimenez, J. L., Livingston, J. M., Redemann, J., Dubovik, O., and Strawa, A.: Absorption Angstrom Exponent in AERONET and related data as an indicator of aerosol composition, Atmos. Chem. Phys., 10, 1155–1169, doi:10.5194/acp-10-1155-2010, 2010.

Saha, A., Mallet, M., Dubuisson, P., Piazzola, J., and Despiau, S.: One year measurements of aerosol optical properties over an urban coastal site: effect on local direct radiative forcing, Atmos. Res. 90, 195–202, doi:10.1016/j.atmosres.2008.02.003, 2008.

Sanchez-Gomez, E., Somot, S., and Mariotti, A.: Future changes in the Mediterranean water budget projected by an ensemble of regional climate models, Geophys. Res. Lett., 36, L21401, doi:10.1029/2009GL040120, 2009.

Sciare, J., Cachier, H., Oikonomou, K., Ausset, P., Sarda-Estève, R., and Mihalopoulos, N.: Characterization of carbonaceous aerosols during the MINOS campaign in Crete, July–August 2001: a multi-analytical approach, Atmos. Chem. Phys., 3, 1743–1757, doi:10.5194/acp-3-1743-2003, 2003.

Sciare, J., Oikonomou, K., Favez, O., Liakakou, E., Markaki, Z., Cachier, H., and Mihalopoulos, N.: Long-term measurements of carbonaceous aerosols in the Eastern Mediterranean: evidence of long-range transport of biomass burning, Atmos. Chem. Phys., 8, 5551–5563, doi:10.5194/acp-8-5551-2008, 2008.

Sciare, J., d'Argouges, O., Sarda Estève, R., Gaimoz, C., Dolgorouky, C., Bonnaire, N., Favez, O., Bonsang, B., and Gros, V.: Large contribution of water-insoluble secondary organic aerosols in the region of Paris (France) during wintertime, J. Geophys. Res., 116, D22203, doi:10.1029/2011JD015756, 2011.

Smirnov, A., Holben, B. N., Eck, T. F., Dubovik, O., and Slutsker, I.: Cloudscreening and quality control algorithms for the AERONET database, Remote Sens. Environ., 73, 337–349, 2000.

Solmon, F., Mallet, M., Elguindi, N., Giorgi, F., Zakey, I., and Konaré, A.: Dust impact on sahelian precipitation gradients, mechanisms and sensitivity to absorption properties, Geophys. Res. Lett., 35, L24705, doi:10.1029/2008GL035900, 2008.

Sun, H., Biedermann, L., and Bond, T. C.: Color of brown carbon: a model for ultraviolet and visible light absorption by organic carbon aerosol, Geophys. Res. Lett., 34, L17813, doi:10.1029/2007GL029797, 2007.

Tafuro, A. M., Kinne, S., De Tomasi, F., and Perrone, M. R.: Annual cycle of direct radiative effect over Southeast Italy and sensitivity studies, J. Geophys. Res., 112, D20202, doi:10.1029/2006JD008265, 2007.

Tanré, D., Kaufman, Y. J., Herman, M., and Mattoo, S.: Remote sensing of aerosol properties over oceans using the MODIS/EOS spectral radiances, J. Geophys. Res., 102, 16971–16988, 1997.

Torres, O., Bhartia, P. K., Herman, J. R., Ahmad, Z., and Gleason, J.: Derivation of aerosol properties from satellite measurements of backscattered ultraviolet radiation: theoretical basis, J. Geophys. Res., 103, 17099–17110, 1998.

Torres, O., Tanskanen, A., Veihelmann, B., Ahn, C., Braak, R., Bhartia, P. K., Veefkind, P., and Levelt, P.: Aerosols and surface UV products from Ozone Monitoring Instrument observations: an overview, J. Geophys. Res., 112, D24S47, doi:10.1029/2007JD008809, 2007.

Valenzuela, A., Olmo, F. J., Lyamani, H., Antón, M., Quirantes, A., and Alados-Arboledas, L.: Classification of aerosol radiative properties during African desert dust intrusions over southeastern Spain by sector origins and cluster analysis, J. Geophys. Res., 117, D06214, doi:10.1029/2011JD016885, 2012.

Wells, K. C., Martins, J. V., Remer, L. A., Kreidenweis, S. M., and Stephens, G. L.: Critical reflectance derived from MODIS: application for the retrieval of aerosol absorption over desert regions, J. Geophys. Res., 117, D03202, doi:10.1029/2011JD016891, 2012.

Yue, X., Liao, H., Wang, H. J., Li, S. L., and Tang, J. P.: Role of sea surface temperature responses in simulation of the climatic effect of mineral dust aerosol, Atmos. Chem. Phys., 11, 6049–6062, doi:10.5194/acp-11-6049-2011, 2011.

Zhang, J. and Reid, J. S.: A decadal regional and global trend analysis of the aerosol optical depth using a data-assimilation grade over-water MODIS and Level 2 MISR aerosol products, Atmos. Chem. Phys., 10, 10949–10963, doi:10.5194/acp-10-10949-2010, 2010.

Table 1. Mediterranean AERONET sites used in this study (classified by latitude). Mean level 2 Aerosol Optical Depth at 440 nm (AOD_{440}) and Angström Exponent between 440 and 870 nm ($AE_{440-870}$) are also indicated. Dominant aerosol types are classified using three different classes: R (Remote), UI (Urban-Industrialized) and D (Dust).

Aeronet/photons site name	Latitude (°N)	Longitude (°E)	Altitude (m)	Period (level 2)	Nr. of observation days (level 2)	Basin (west/east)	Site characteristics	AOD_{440}	$AE_{440-870}$	Dominant aerosol type
Modena (MOD)	44.63	10.94	56	May 2000 → Nov 2011	1300	West	Urban	0.32	1.55	UI
Avignon (AVI)	43.93	4.87	32	Jan 2000 → Sep 2012	3017	West	Rural	0.20	1.47	UI
Villefranche-sur-Mer (VSM)	43.68	7.33	130	Feb 2004 → Mar 2012	1538	West	Peri-urban coastal	0.20	1.49	UI
Toulon (TLN)	43.13	6.00	50	Feb 2005 → Jul 2010	1580	West	Urban coastal	0.16	1.48	UI
Ersa (ERS)	43.00	9.35	80	Jun 2008 → Sep 2011	869	West	Remote island	0.16	1.43	R
Rome Tor Vergata (ROM)	41.84	12.65	130	Oct 2001 → Jul 2011	2236	West	Peri-urban	0.21	1.41	UI
Barcelone (BCN)	41.38	2.17	125	Mar 2005 → Mar 2011	1855	West	Urban near coastal	0.19	1.42	UI
Thessaloniki (THS)	40.63	22.96	60	Sep 2005 → Nov 2010	982	East	Urban coastal	0.28	1.57	UI
IMAA-Potenza (POT)	40.60	15.72	820	Aug 2006 → Sep 2011	1076	West	Urban	0.15	1.36	UI
Lecce University (LEC)	40.33	18.11	30	Apr 2003 → Aug 2010	1791	East	Peri-urban coastal	0.21	1.35	UI
Oristano (ORI)	39.91	8.5	10	Jun 2000 → Oct 2003	934	West	Peri-urb. coastal	0.21	1.21	UI-D
Burjassot (BUR)	39.50	−0.42	30	Apr 2007 → Oct 2011	1102	West	Urban near coastal	0.18	1.32	UI
Messina (MES)	38.20	15.57	15	May 2005 → Jun 2011	958	West	Urban coastal	0.22	1.31	UI
Athens-NOA (ATH)	37.99	23.77	130	May 2008 → Nov 2010	878	East	Urban coastal	0.21	1.37	UI
Granada (GRA)	37.16	−3.6	680	Feb 2005 → Oct 2011	1493	West	Urban	0.17	1.23	UI-D
Malaga (MAL)	36.71	−4.47	40	May 2009 → Oct 2011	830	West	Peri-urban	0.16	1.11	UI-D
IMS-METU-Erdemli (ERD)	36.56	34.25	3	Mar 2000 → Oct 2011	2176	East	Rural coastal	0.28	1.27	R-D
Blida (BLI)	36.50	2.88	230	Feb 2004 → Nov 2009	1645	West	Rural coastal	0.22	1.03	D
Lampedusa (LAM)	35.51	12.63	45	Jun 2003 → Jun 2011	1217	East	Remote Island	0.19	1.00	D
Forth Crete (FOR)	35.33	25.28	20	Mar 2003 → Jul 2009	2207	East	Remote Island	0.21	1.16	R-D
Nes Ziona (NZI)	31.92	34.78	40	Jul 2000 → Apr 2011	2321	East	Peri-urban coastal	0.29	0.98	R-D
Sede Boker (SED)	30.85	34.78	480	Apr 1996 → Apr 2012	4150	East	Rural semi-arid	0.21	0.92	R-D

Table 2. Level-2 averaged Aerosol Absorbing Optical Depth at 440 nm ($AAOD_{440}$), Single Scattering Albedo at 440 nm (SSA_{440}), Absorbing Angström Exponent estimated between 440 and 870 nm ($AAE_{440-870}$), real and imaginary parts of aerosol Refractive Index (RI) at 440 and 670 nm, and number of days with data over the time period reported in Table 1. Standard deviations (sigma) are also reported in parentheses for AOD, SSA and AAE.

Aeronet/photons Site	$AAOD_{440}$ (sigma)	SSA_{440} (sigma)	$AAE_{440-870}$ (sigma)	Real part of RI at 440/670 nm	Imaginary part of RI at 440/670 nm (×10 000)
Modena	0.036 (0.014)	0.930 (0.026)	1.28 (0.21)	1.43/1.43	97/86
Avignon	0.039 (0.012)	0.918 (0.023)	1.24 (0.37)	1.42/1.43	98/89
Villefranche-sur-Mer	0.024 (0.012)	0.951 (0.024)	0.99 (0.24)	1.40/1.41	55/58
Toulon	0.033 (0.015)	0.929 (0.034)	1.20 (0.32)	1.40/1.42	90/87
Ersa	0.023 (0.014)	0.955 (0.023)	1.16 (0.28)	1.41/1.42	55/56
Rome Tor Vergata	0.047 (0.021)	0.904 (0.042)	1.50 (0.43)	1.43/1.44	119/89
Barcelone	0.036 (0.017)	0.929 (0.027)	1.19 (0.48)	1.42/1.42	74/65
Thessaloniki	0.031 (0.010)	0.937 (0.020)	1.33 (0.19)	1.38/1.40	69/57
Potenza	0.039 (0.023)	0.925 (0.040)	1.28 (0.63)	1.45/1.46	73/75
Lecce University	0.036 (0.014)	0.925 (0.026)	1.47 (0.53)	1.44/1.45	76/64
Oristano	0.056 (0.041)	0.907 (0.023)	1.59 (0.50)	1.44/1.46	70/46
Burjassot	0.030 (0.012)	0.939 (0.021)	1.18 (0.29)	1.43/1.42	59/51
Messina	0.037 (0.025)	0.933 (0.031)	1.20 (0.39)	1.42/1.43	62/58
Athens-NOA	0.043 (0.007)	0.906 (0.015)	1.45 (0.42)	1.43/1.43	106/89
Granada	0.048 (0.017)	0.904 (0.031)	1.71 (0.51)	1.43/1.46	63/37
Malaga	0.048 (0.015)	0.898 (0.028)	1.61 (0.42)	1.43/1.46	65/41
Erdemli	0.040 (0.025)	0.922 (0.048)	1.18 (0.43)	1.41/1.42	73/59
Blida	0.055 (0.020)	0.896 (0.031)	1.80 (0.42)	1.43/1.46	79/46
Lampedusa	0.037 (0.019)	0.929 (0.030)	2.13 (0.65)	1.46/1.48	35/18
Forth Crete	0.038 (0.022)	0.928 (0.019)	1.68 (0.45)	1.43/1.45	49/33
Nes Ziona	0.052 (0.036)	0.902 (0.071)	1.45 (0.56)	1.44/1.44	97/58

Table 3. Description of the three different sensors used for characterizing aerosol column SSA. The wavelength used for each sensor in this study is bold.

Sensor	λ (nm)	Horizontal resolution	Retrieval	Period
MISR	446, **558**, 672 and 866	0.5° × 0.5°	Land/Sea (Kahn et al., 2010)	2000 → 2011
MODIS (Deep Blue product)	412, **470** and 660	1° × 1°	High reflectance surface only (see Hsu et al., 2004, 2006)	2005 → 2011
OMI	388, **500**	1° × 1°	Land/Sea	2005 → 2008

Table 4. Adjusted parameters of particle volume size distributions averaged for the stations relevant to the western and eastern basins (see Fig. 9), assuming bimodal lognormal distributions (R is the modal radius and σ_g the geometric standard deviation).

Basin	Western		Eastern	
mode	Fine	Coarse	Fine	Coarse
Proportion (%)	37.0	63.0	30.6	69.4
R (μm)	0.158	2.34	0.157	2.23
σ_g	1.61	2.11	1.58	2.02

Fig. 1. Location of the 22 Mediterranean AERONET sites with long time series used in this work. Northernmost (resp. southernmost) sites are found in the western (eastern) basin.

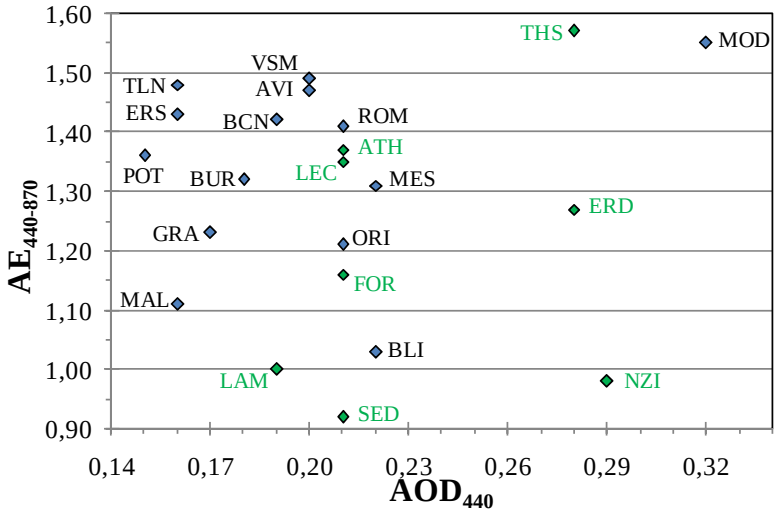

Fig. 2. Average AERONET level 2 aerosol Angström Exponent and optical depth of the 22 selected stations. The 8 stations in green are relevant of the eastern Basin (see Table 1 for the station codes).

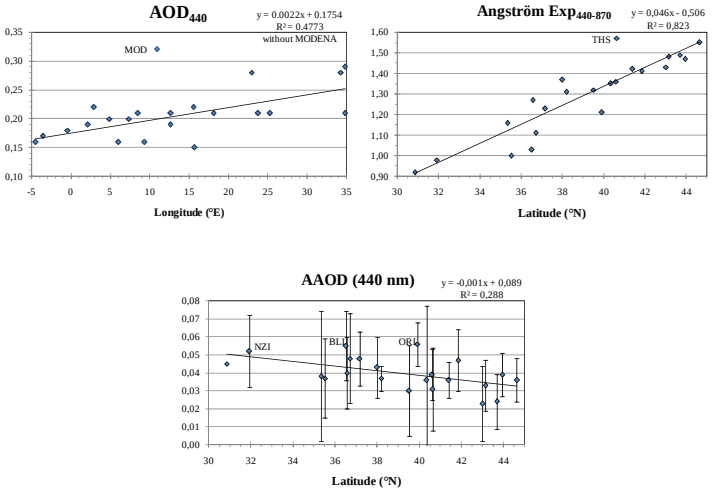

Fig. 3. AERONET level-2 average AOD as a function of station longitude and average AE and AAOD as a function of station latitude. Other data given in Table 2 are less or not significantly correlated with latitude or longitude with the exception of the real part of RI at 440 and 670 nm and the imaginary part of RI at 670 nm (not shown) that also correlate with latitude at the 0.01 level ($R^2 > 0.288$ for 20 degrees of freedom).

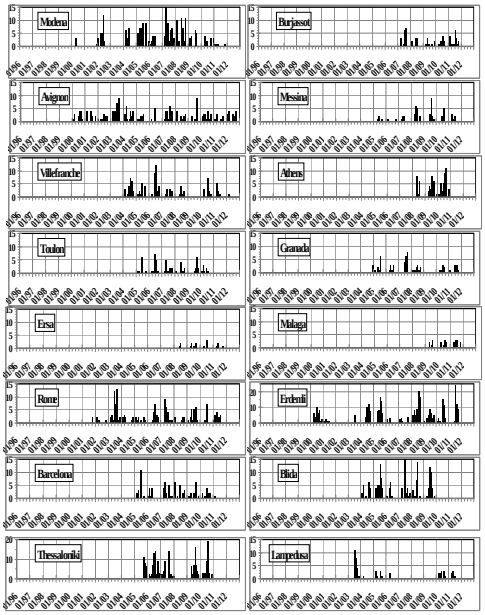

Fig. 4. Number of days with available level-2 AAOD (at 440 or 441 nm) data at every AERONET station and for each month from January 1996 to December 2012. Note that Thessaloniki and Erdemli have vertical scales different from other stations. Similar figures for Potenza, Forth Crete, Lecce, Nes Ziona, Oristano and Sede Boker are provided as annexe material.

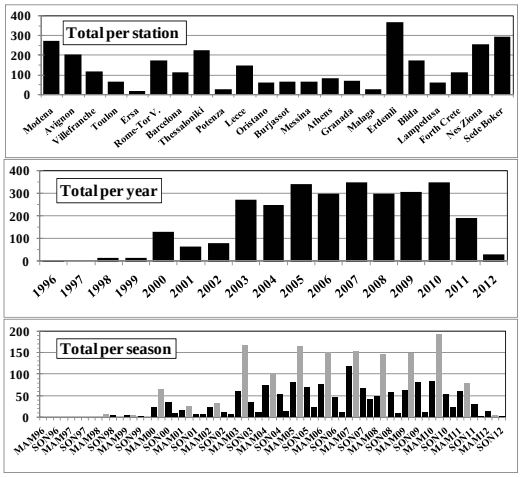

Fig. 5. Total number of days with available level-2 AAOD (at 440 or 441 nm) data per station (top), and per year (middle) and per season (bottom, with summer seasons in grey) for stations altogether.

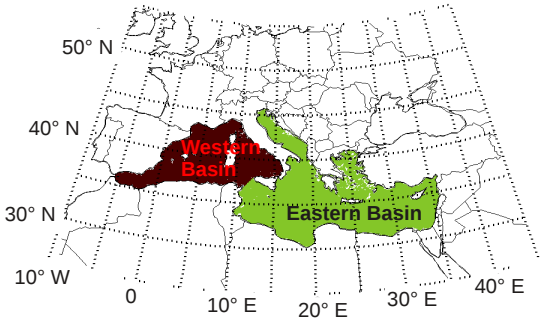

Fig. 6. Sub-Mediterranean basin integration area for MISR and OMI SSA products.

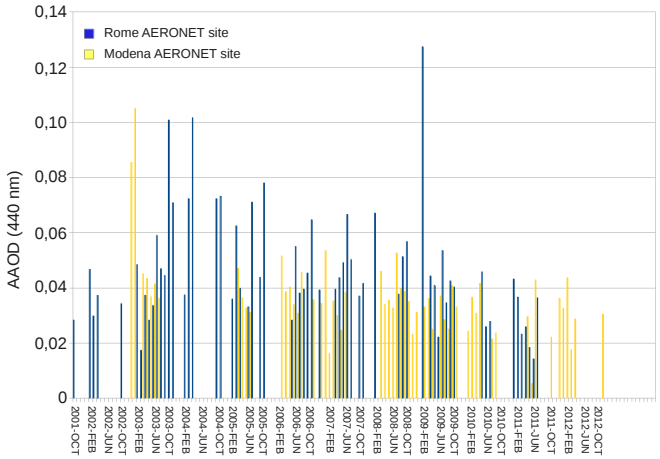

Fig. 7. Absorbing Aerosol Optical Depth, AAOD (level 2, at 440 nm) estimated at Rome and Modena for the 2001 to 2012 period. The uncertainty is about ±0.01.

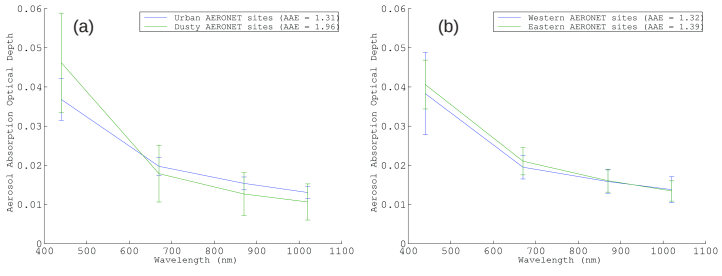

Fig. 8. Wavelength dependence of Aerosol Absorbing Optical Depth (AAOD) for Urban-Industrialised and Dusty AERONET sites **(a)** and for Western and Eastern AERONET sites **(b)**. Associated mean AAE (calculated between 440 and 880 nm) and standard deviations are also reported.

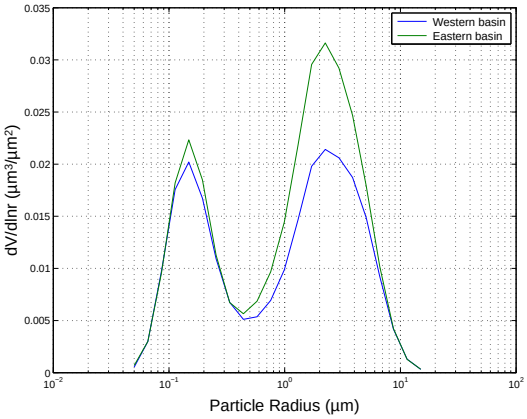

Fig. 9. AERONET level-2 aerosol volume size distribution averaged over the 8 eastern and 14 western sites (see Table 1). Inversion is performed in 22 logarithmically equidistant size bins between 0.05 and 15 µm in radius. Adjusted parameters are given in Table 4.

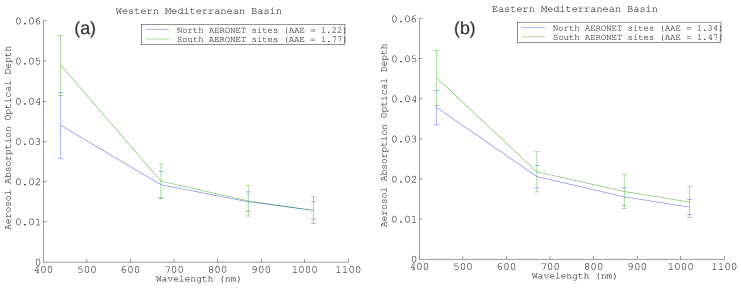

Fig. 10. Wavelength dependence of Aerosol Absorbing Optical Depth (AAOD) for Northern and Southern AERONET sites classified over the **(a)** Western and **(b)** Eastern basins. Associated mean AAE (calculated between 440 and 880 nm) and standard deviations are also reported.

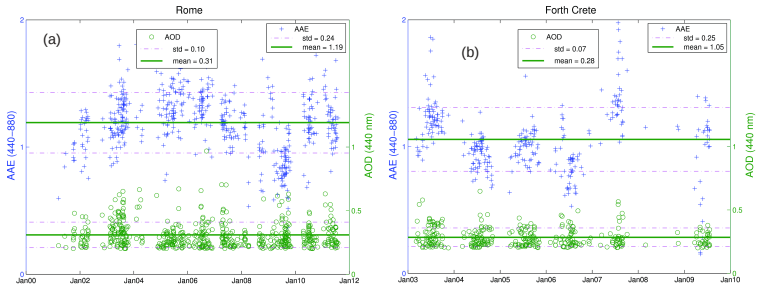

Fig. 11. AAE (calculated between 440 and 870 nm) and AOD (440 nm) estimated from AERONET level 1.5 data for Rome **(a)** and Crete **(b)** AERONET sites. Mean values and standard deviations are included.

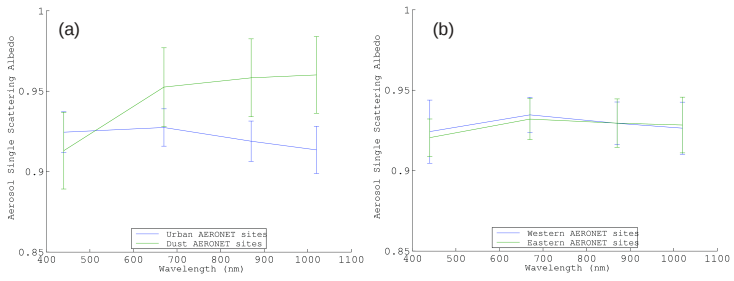

Fig. 12. Wavelength dependence of Single Scattering Albedo (SSA) for Urban and Dusty AERONET sites **(a)** and for Western and Eastern AERONET sites **(b)**. Standard deviations are also reported.

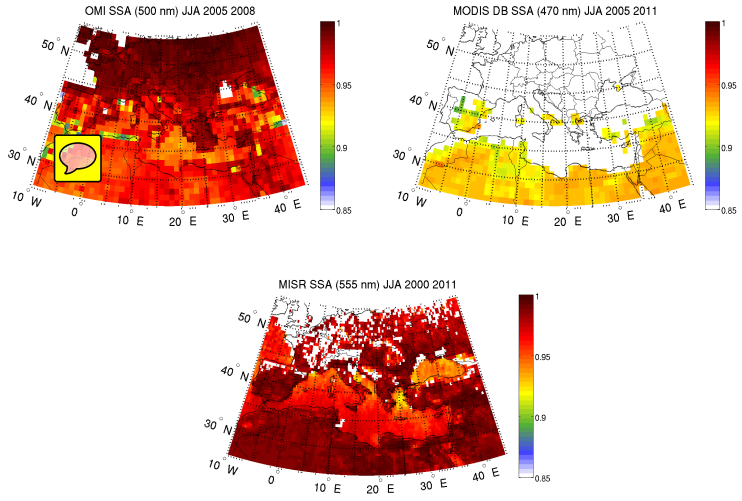

Fig. 13. Averaged summer (June-July-August, JJA) SSA estimated over the Mediterranean using OMI (2005–2008), MODIS Deep Blue (2005–2011) and MISR (2000–2011) satellite products.

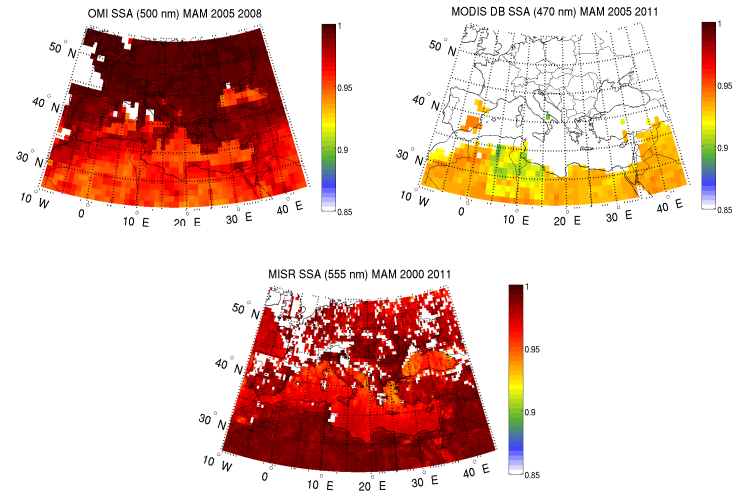

Fig. 14. Averaged Spring (March-April-May, MAM) SSA estimated over the Mediterranean using OMI (2005–2008), MODIS Deep Blue (2005–2011) and MISR (2000–2011) satellite products.

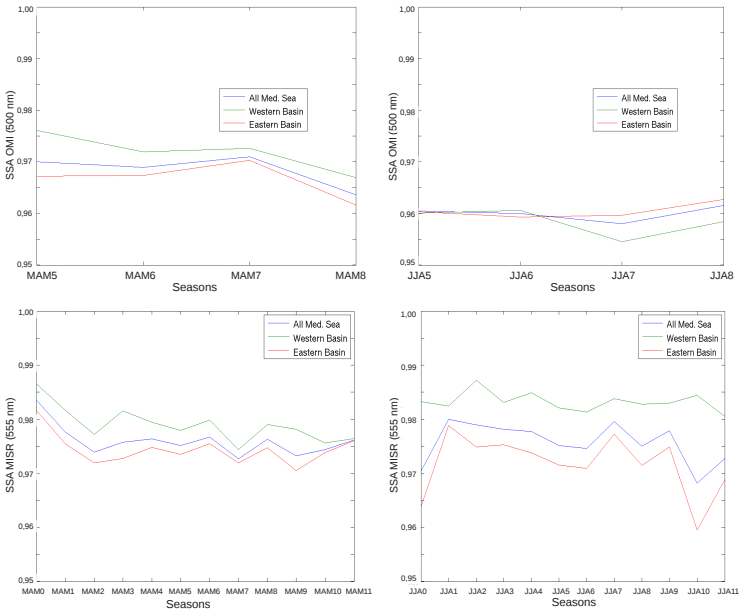

Fig. 15. Mean spring (MAM, left column) and summer (JJA, right column) SSA estimated from OMI (500 nm, top) and MISR (558 nm, bottom) over all the Mediterranean (blue line), eastern (red line) and western (green line) basins as defined in Fig. 6.